Volume: 2 Issue: 3 Pages: 50-54

Composition-Dependent Structural Properties of $Bi_2Te_{3x}Se_{3(1-x)}$ Ternary Thin Films

[*1] G.D. Deshmukh

[*1] Associate Professor, Department of Physics, Nanasaheb Y. N. Chavan Arts, Science and Commerce College, Chalisgaon, Jalgaon, India.

Article Info.
E-ISSN: 2583-6528
Impact Factor (SJIF): 5.231
Available online:
www.alladvancejournal.com

Received: 26/Feb/2023
Accepted: 24/Mar/2023

***Corresponding Author**
G.D. Deshmukh
Associate Professor, Department of Physics, Nanasaheb Y. N. Chavan Arts, Science and Commerce College, Chalisgaon, Jalgaon, India.

Abstract
Ternary bismuth telluride-selenide ($Bi_2Te_{3x}Se_{3(1-x)}$) thin films have emerged as promising materials for thermoelectric and topological insulator applications due to their tunable electronic and structural properties. This study investigates the composition-dependent structural evolution of $Bi_2Te_{3x}Se_{3(1-x)}$ thin films across the complete compositional range ($0 \leq x \leq 1$). X-ray diffraction analysis reveals that these ternary alloys maintain the rhombohedral structure represented in the hexagonal lattice strongly orientated along (1010) direction. The difference in d-values and lattice parameter values '*a*' with composition obeys Vegard's law. The structural parameters such as grain size, microstrain and dislocation density are fairly depending on composition. The grain size observed is about 25-50 nm. These findings provide fundamental insights into the structure-composition relationships essential for advancing applications in next-generation thermoelectric devices and quantum electronics.

Keywords: Bismuth telluride, bismuth selenide, ternary alloys, thin films, structural properties, thermoelectric materials, topological insulators.

Introduction

Thermoelectric materials, capable of directly converting heat energy into electrical energy and vice versa, have garnered significant attention due to their potential in waste heat recovery and solid-state cooling applications [1]. The efficiency of such materials is quantified by the dimensionless figure of merit, $ZT = (S^2\sigma T)/\kappa$, where S is the Seebeck coefficient, σ is the electrical conductivity, T is the absolute temperature, and κ is the total thermal conductivity [2]. Optimizing ZT typically involves enhancing the power factor ($S^2\sigma$) while simultaneously reducing the thermal conductivity, a challenge given the interdependencies of these parameters [3]. The binary compounds such as Bi_2Te_3, Bi_2Se_3 and Sb_2Te_3 in the family of V-VI compounds are narrow band semiconductors and found to be highly efficient thermoelectric materials around room temperature [4]. The V-VI chalcogenides and their mixed ternary compounds $Bi_2Te_{3x}Se_{3\ (1-x)}$ ($0 \leq x \leq 1$) have semi-conducting properties, which are especially suitable for the small scale power generators, detectors, low weight refrigerators etc. [5]. The research on $Bi_2Te_{3x}Se_{3(1-x)}$ semiconductors started with great interest to understand the physical properties of these materials. These semiconductors exist in layered crystal structure leads to a poor thermal conductivity, making most suitable for thermoelectric applications [6]. In the specific case of $Bi_2Te_{3x}Se_{3(1-x)}$ due to the isomorphic crystal structure of Bi_2Te_3 and Bi_2Se_3, the solubility of Se in Bi_2Te_3 results in the modification of the crystalline structure and electronic density of states, which is beneficial for inhibiting the onset of intrinsic conduction and is an important factor for the thermoelectric properties of Bi_2Te_3 alloys [7].

Experimental

Using Bi_2Te_3 and Bi_2Se_3 powder (Sigma-Aldrich 99.99+ % purity) the ternary thin films of $Bi_2Te_{3x}Se_{3(1-x)}$ (x = 0.1 to 0.9) were deposited by means of sublimation of the compound onto well cleaned glass substrates by thermal evaporation in vacuum ($\approx 10^{-5}$ torr) using molybdenum boat as a source. In order to prepare ternary semiconductors of $Bi_2Te_{3x}Se_{3(1-x)}$ (x = 0.1 to 0.9) the constituent compounds of Bi_2Te_3 and Bi_2Se_3 have been taken in molecular stoichiometry proportional weights, crushed and mixed homogenously. The different sets of samples of varying compositions (x = 0.1 to 0.9) with different thicknesses for the ternaries were deposited under

controlled growth conditions. The rate of deposition and thickness of the films were controlled by using quartz crystal thickness monitor model no. DTM-101 provided by HINDHIVAC. The deposition rate was maintained 3–5 Å/sec constant throughout the sample preparations. The film thicknesses were confirmed by using weight-difference method with the help of digital balance (DENOVER- Model: TB-214, Germany) having accuracy of 0.1mg. The source to substrate distance was kept constant (14 cm). The alumel-chromel thermocouple placed in contact with the substrates continuously records the substrate temperature (≈ 306 K). Deposited samples were kept under vacuum overnight. The selected samples of $Bi_2Te_{3x}Se_{3(1-x)}$ (x = 0.1 to 0.9) thin films having nearly equal thicknesses (≈ 2500 Å) were used for the study. These samples were annealed at 423 K for 30 min. in vacuum (≈10^{-5} torr) and used for the characterization.

Result and Dicussion

Characterization

The X-ray diffraction (XRD) patterns of selected $Bi_2Te_{3x}Se_{3(1-x)}$ annealed samples were recorded by X-ray diffractometer (Bruker, model D-8 Advance) with CuKα radiation (1.5406 Å). The surface morphology and the chemical composition of these films were investigated by field emission scanning electron microscope (FESEM) attached with EDAX using model Hitachi S-4800-II (Japan).

Structural Analysis

The X-ray diffraction patterns of the thermally evaporated $Bi_2Te_{3x}Se_{3(1-x)}$ (x = 0.1 to 0.9) thin films of thickness 2500 Å annealed at 423 K for 30 min. in vacuum (≈10^{-5} torr) are shown in Fig.1.

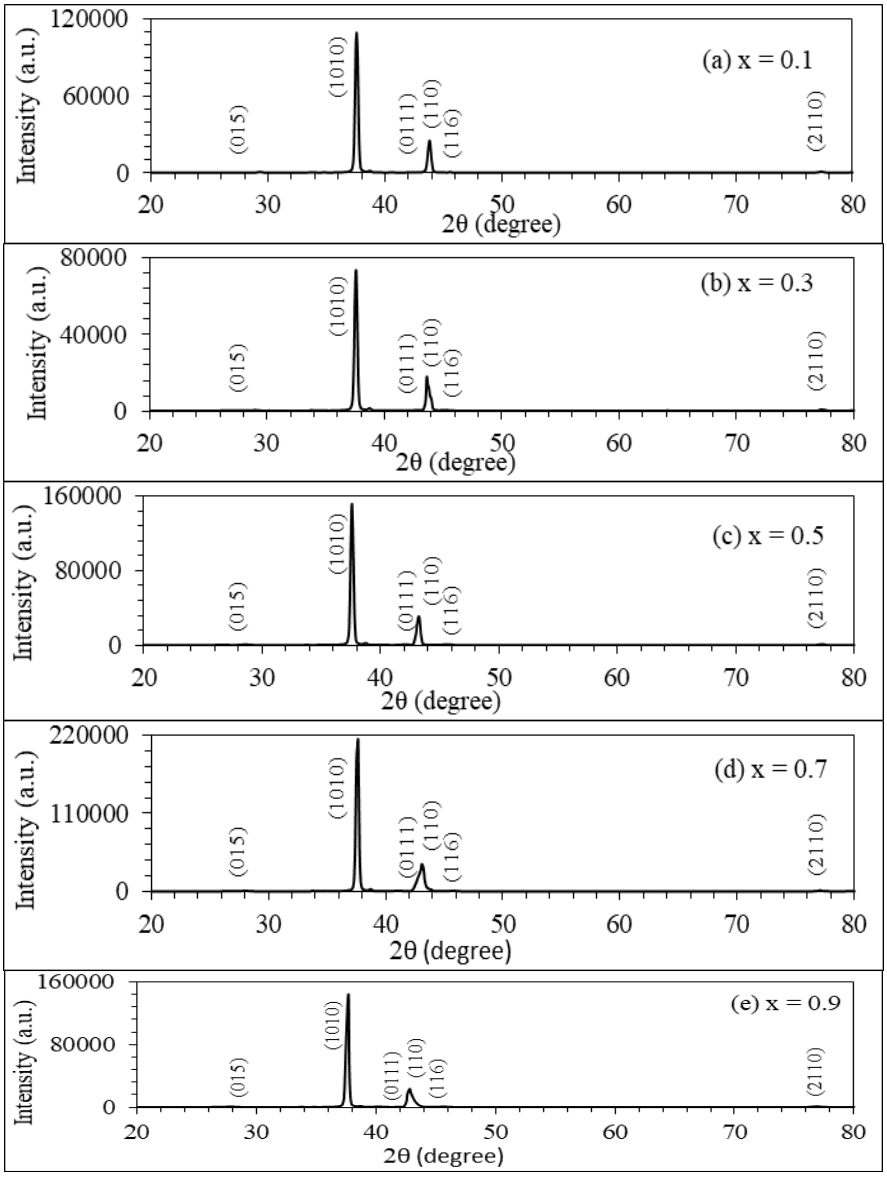

Fig 1: XRD patterns of $Bi_2Te_{3x}Se_{3(1-x)}$ thin films annealed at 423 K for 30 min in vacuum (≈ 10^{-5} torr)

These XRD patterns shows that, all the films are polycrystalline exhibiting rhombohedral structure which is usually represented in the hexagonal lattice, with strong preferential orientation of the crystallites along (1010) direction for all the compositions. The same results are reported by V. D. Das and S. Selvaraj (2000), D. H. Park *et al* (2011) and S. M. Patil *et al* (2012) for $Bi_2Te_{3x}Se_{3(1-x)}$ thin films [8-10]. These samples also show lower intensity peaks for (015), (0111), (116) and (2110) directions. It is observed that the intensity of peaks is maximum for the film with composition x = 0.7, while it is minimum for x = 0.3. The intensity of peaks increases from composition x = 0.1 to x = 0.7 except x = 0.3, then it decreases up to x = 0.9.The experimental d-values for the different compositions of $Bi_2Te_{3x}Se_{3(1-x)}$ ternary system are calculated using the Bragg's law for each composition along the prominent peak

corresponding to (1010) rhombohedral structure and compared with the standard American Standard for Testing and Materials (ASTM) data card d-values (d*) obtained from Vegard's law for $Bi_2Te_{3x}Se_{3(1-x)}$ system.

According to Vegard's law, the d* for ternary system will be the linear function of concentrations of the constituent crystals [20] for $CdSe_xTe_{1-x}$ and are expressed for $Bi_2Te_{3x}Se_{3(1-x)}$ ternary system as,

$$d^* = (x)\, d(Bi_2Te_3) + (1\text{-}x)\, d(Bi_2Se_3)$$

The standard JCPDS data of Bi_2Te_3 (Card No. 15-0863) and Bi_2Se_3 (Card No. 33-0214) is correlated. The comparison of standard d-values (d*) and observed d-values for different compositions of $Bi_2Te_{3x}Se_{3(1-x)}$ (x = 0.1 to 0.9) thin films is given in Table 1(a) to (c).The observed d-values are in good agreement with the standard d-values.

Table 1 (a): The comparison of standard (d*) and observed d-values

Standard	Observed			Standard	Observed			Standard	Observed		
(x = 0.1)	(x = 0.1)			(x = 0.2)	(x = 0.2)			(x = 0.3)	(x = 0.3)		
d*	2θ	d-value	Int.	d*	2θ	d-value	Int.	d*	2θ	d-value	Int.
3.0582	29.24	3.0518	1	3.0764	29.08	3.0682	1	3.0946	29	3.0765	1
2.3760	37.58	2.3915	100	2.3760	37.62	2.3890	100	2.3760	37.58	2.3915	100
2.1192	42.83	2.1097	1	2.1324	42.8	2.1111	1	2.1456	42.74	2.1139	1
2.0822	43.82	2.0643	23	2.0944	43.68	2.0706	23	2.1066	43.61	2.0738	24
1.9111	45.59	1.9882	1	1.9224	45.36	1.9977	1	1.9338	45.36	1.9977	1
1.2319	77.36	1.2325	1	1.2393	77.36	1.2325	1	1.2467	77.2	1.2347	1

Table 1 (b): The comparison of standard (d*) and observed d-values

Standard	Observed			Standard	Observed			Standard	Observed		
(x = 0.4)	(x = 0.4)			(x = 0.5)	(x = 0.5)			(x = 0.6)	(x = 0.6)		
d*	2θ	d-value	Int.	d*	2θ	d-value	Int.	d*	2θ	d-value	Int.
3.1128	28.49	3.1304	1	3.1310	28.49	3.1304	1	3.1492	28.25	3.1565	1
2.3760	37.64	2.3878	100	2.3760	37.58	2.3915	100	2.3760	37.62	2.3890	100
2.1588	42.48	2.1263	1	2.1720	42.02	2.1485	1	2.1852	41.95	2.1519	1
2.1188	43.49	2.0792	24	2.1310	43.22	2.0916	22	2.1432	43.19	2.0930	18
1.9451	45.72	1.9829	1	1.9564	45.74	1.9820	1	1.9677	45.74	1.9820	1
1.2541	77.21	1.2346	1	1.2616	77.3	1.2333	1	1.2690	77.24	1.2342	1

Table 1 (c): The comparison of standard (d*) and observed d-values

Standard	Observed			Standard	Observed			Standard	Observed		
(x = 0.7)	(x = 0.7)			(x = 0.8)	(x = 0.8)			(x = 0.9)	(x = 0.9)		
d*	2θ	d-value	Int.	d*	2θ	d-value	Int.	d*	2θ	d-value	Int.
3.1674	28.12	3.1708	1	3.1856	27.94	3.1908	1	3.2038	27.78	3.2088	1
2.3760	37.65	2.3872	100	2.3760	37.68	2.3854	100	2.3760	37.68	2.3854	100
2.1984	41	2.1996	1	2.2116	40.25	2.2388	1	2.2248	40.22	2.2404	1
2.1554	43.09	2.0976	18	2.1676	42.98	2.1027	18	2.1798	42.82	2.1102	16
1.9790	45.7	1.9837	1	1.9904	45.7	1.9837	1	2.0017	45.66	1.9853	1
1.2764	77.12	1.2358	1	1.2838	77.01	1.2373	1	1.2912	76.9	1.2388	1

The lattice parameter 'a' corresponding to (1010) rhombohedral structure, usually represented in the hexagonal lattice has been evaluated from the relation [8, 11].

$$\frac{1}{d^2} = \left(\frac{4}{3}\right)\left(\frac{h^2 + hk + k^2}{a^2}\right) + \frac{l^2}{c^2} \quad (1)$$

where 'd' is the atomic spacing value and h, k, and l are the Miller indices.

The grain or crystallite size is determined by using Scherrer formula

$$\text{Grain size (D)} = \frac{k\lambda}{\beta\cos\theta} \quad (2)$$

where the constant 'k' is a shape factor usually ≈ 0.94, λ is the wavelength of the X-ray (1.5406 Å), θ is the Bragg's angle and β is the full-width half-maximum (FWHM).The microstrain (ε) developed in the film was calculated from the slope of

β cosθ versus sinθ plot [12, 13] using the relation

$$\beta = \left(\frac{\lambda}{D\cos\theta}\right) - (\varepsilon \tan\theta) \quad (3)$$

The dislocation density (δ), defined as the length of dislocation lines per unit volume of the crystal, was evaluated from the formula

$$\delta = \frac{1}{D^2} \quad (4)$$

The grain size (D), microstrain (ε) and dislocation density (δ) for all the compositions of $Bi_2Te_{3x}Se_{3(1-x)}$ along (1010) rhombohedral phase have been calculated using above formulae and the values are specified in the Table 2.

Table 2: Calculated structural parameters for the (1010) rhombohedral phase of $Bi_2Te_{3x}Se_{3(1-x)}$ thin films annealed at 423K for 30 min. in vacuum (≈10^{-5} torr)

Composition (x)	2θ (°)	FWHM (β) (°)	Grain size (D) (nm)	Microstrain (ε x 10^{-4}) (lines^{-2} m^{-4})	Dislocation density (δ x 10^{13}) (lines/m^2)
0.1	37.58	0.282	31.09	11.65	103
0.2	37.62	0.283	30.98	11.69	104
0.3	37.58	0.284	30.87	11.73	105
0.4	37.64	0.283	30.98	11.69	104
0.5	37.58	0.283	30.98	11.69	104
0.6	37.62	0.286	30.65	11.81	106
0.7	37.65	0.287	30.55	11.90	107
0.8	37.68	0.284	30.88	11.70	105
0.9	37.68	0.280	31.32	11.60	102

From Table 2 it is seen that for the composition x = 0.9, FWHM, microstrain and dislocation density all are minimum, while the same parameters are maximum for the composition x = 0.7. These all tend to oscillates from the composition x = 0.1 to x = 0.9. It is observed that the grain size is lower for the compositions with x = 0.7, the variation in grain size for different compositions is very small.

The average lattice parameters (a) are evaluated from the XRD data of the films and they agreed well with the previous reports. Vegard's Law is used for the estimation of the standard lattice parameters (*astandard*) for all compositions.

$$a_{standard} = (x)\, a(Bi_2Te_3) + (1\text{-}x)\, a(Bi_2Se_3) \quad (5)$$

The comparison of standard and observed lattice parameters for different compositions (x) is given in Table 3. Both the values are found to be in good agreement.

Table 3: Comparison of standard and observed lattice parameters (a) for annealed $Bi_2Te_{3x}Se_{3(1-x)}$ thin films

Composition x	Standard 'a'	Observed 'a'
0.1	4.1642	4.1655
0.2	4.1887	4.1892
0.3	4.2133	4.2129
0.4	4.2378	4.2366
0.5	4.2624	4.2603
0.6	4.2870	4.2840
0.7	4.3115	4.3077
0.8	4.3361	4.3315
0.9	4.3606	4.3552

FESEM analysis

The field emission scanning electron microscope images of $Bi_2Te_{3x}Se_{3(1-x)}$ thin films of different compositions are shown in Fig. 2. The images show that the deposited films are having uniform deposition, homogeneous surface and are polycrystalline in nature. All films illustrate well adherent, uniform film surface without cracks and good crystallanity. The grain size observed from the FESEM images is about 25-50 nm.

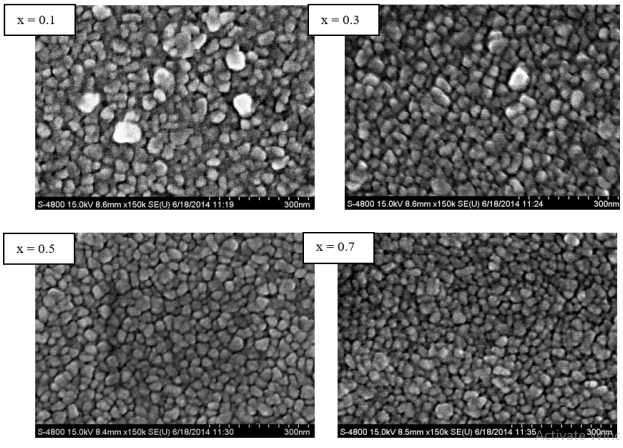

Fig 2: FESEM micrographs of thermally evaporated annealed $Bi_2Te_{3x}Se_{3(1-x)}$ films of different compositions

Conclusion

The ternary thin films of $Bi_2Te_{3x}Se_{3(1-x)}$ of compositions x = 0.1 to 0.9 were deposited onto glass substrates by thermal evaporation and annealed at 423 K for 30 min. in vacuum. The XRD patterns indicates that, for all the compositions films are polycrystalline exhibiting rhombohedral structure represented in the hexagonal lattice strongly orientated along (1010) direction. The variation in d-values and lattice parameter values '*a*' with composition obeys Vegard's law. The structural parameters such as grain size, microstrain and dislocation density are fairly depending on composition. The EDAX analysis shows that the films with compositions x = 0.2, 0.7, 0.8 and 0.9 are closely stoichiometric. The films with compositions x = 0.1, 0.4, 0.5 and 0.6 are Bi rich due to difference in vapour pressure of Bi, Te and Se and loss of tellurium due to re-evaporation during annealing. The FESEM images of $Bi_2Te_{3x}Se_{3(1-x)}$ thin films of different compositions shows that the deposited films are polycrystalline in nature, well adherent, uniform film surface without cracks and show decent crystallanity. The grain size observed from the FESEM images are about 25-50 nm.

References

1. Malik K, Mahakal S, Das D, Banerjee A, Chatterjee S, Das A. Sb concentration dependent Structural and Transport properties of Polycrystalline (Bi1-xSbx)2Te3 Mixed crystal. arXiv (Cornell University), 2021. https://doi.org/10.48550/arxiv.2108.00525
2. Wong-Ng W, Yan Y, Martin J, Otani M, Thomas EL, Tang X, Green ML. Development and Applications of Non-destructive Screening Tools for Thermoelectric Materials at NIST. Ferroelectrics. 2014; 470(1):241. https://doi.org/10.1080/00150193.2014.923725
3. Viskadourakis Z, Drymiskianaki A, Papadakis V, Ioannou I, Kyratsi T, Kenanakis G. Thermoelectric Performance of Mechanically Mixed BixSb2-xTe3-ABS Composites. *Materials*. 2021; 14(7):1706. https://doi.org/10.3390/ma14071706
4. Nolas GS, Sharp J, Goldsmid HJ, Thermoelectric Basic Principles and New Materials Developments, Springer, New York, 2001.
5. Arifov YA, Kulagin AI, Erzin NI *et al.* Appl. Solar Energy. 1974; 10:63-65.
6. Rowe DM. Thermoelectrics handbook: Macro to Nano, Taylor and Francis, Boca Raton, FI, 2006.
7. Yu R, Zhang W, Zhang HJ. *et al*., Science. 2010; 329(5987):61-64.
8. Das VD, Selvaraj S. Materials Chemistry and Physics. 2000; 62:68-74.
9. Park DH, Kim MY, Oh TS. Current Applied Physics. 2011; 11:S41-S45.
10. Patil SM, Gavale SN, Mane RK. *et al*., Arch. Phy. Res. 2012; 3(3):245-257.
11. Goswami A. Thin Film Fundamentals, New Age International Pvt. Ltd., 2014, 69.
12. Patil SS, Pawar PH, J. Chem. Bio. Phy. Sci. Sec. C. 2012; 2(3):1472-1484.
13. Velumani S, Mathew X, Sebastain PJ, Sol. Energy Mater. Sol. Cells. 2003; 76:359.